university of groningen

University Medical Center Groningen

University of Groningen

Cytosolic Delivery of Single-Chain Polymer Nanoparticles

Hamelmann, Naomi M.; Paats, Jan Willem D.; Paulusse, Jos M.J.

Published in:
Acs Macro Letters

DOI:
10.1021/acsmacrolett.1c00558

IMPORTANT NOTE: You are advised to consult the publisher's version (publisher's PDF) if you wish to cite from it. Please check the document version below.

Document Version
Publisher's PDF, also known as Version of record

Publication date:
2021

Link to publication in University of Groningen/UMCG research database

Citation for published version (APA):
Hamelmann, N. M., Paats, J. W. D., & Paulusse, J. M. J. (2021). Cytosolic Delivery of Single-Chain Polymer Nanoparticles. *Acs Macro Letters*, *10*(11), 1443-1449. https://doi.org/10.1021/acsmacrolett.1c00558

Copyright
Other than for strictly personal use, it is not permitted to download or to forward/distribute the text or part of it without the consent of the author(s) and/or copyright holder(s), unless the work is under an open content license (like Creative Commons).

The publication may also be distributed here under the terms of Article 25fa of the Dutch Copyright Act, indicated by the "Taverne" license. More information can be found on the University of Groningen website: https://www.rug.nl/library/open-access/self-archiving-pure/taverne-amendment.

Take-down policy
If you believe that this document breaches copyright please contact us providing details, and we will remove access to the work immediately and investigate your claim.

Downloaded from the University of Groningen/UMCG research database (Pure): http://www.rug.nl/research/portal. For technical reasons the number of authors shown on this cover page is limited to 10 maximum.

Download date: 20-11-2022

ACS Macro Letters

pubs.acs.org/macroletters Letter

Cytosolic Delivery of Single-Chain Polymer Nanoparticles

Naomi M. Hamelmann, Jan-Willem D. Paats, and Jos M. J. Paulusse*

Cite This: *ACS Macro Lett.* 2021, 10, 1443−1449 Read Online

ACCESS | Metrics & More | Article Recommendations | Supporting Information

ABSTRACT: Cytosolic delivery of therapeutic agents is key to improving their efficacy, as the therapeutics are primarily active in specific organelles. Single-chain polymer nanoparticles (SCNPs) are a promising nanocarrier platform in biomedical applications due to their unique size range of 5−20 nm, modularity, and ease of functionalization. However, cytosolic delivery of SCNPs remains challenging. Here, we report the synthesis of active ester-functional SCNPs of approximately 10 nm via intramolecular thiol-Michael addition cross-linking and their functionalization with increasing amounts of tertiary amines 0 to 60 mol % to obtain SCNPs with increasing positive surface charges. No significant cytotoxicity was detected in bEND.3 cells for the SCNPs, except when SCNPs with high amounts of tertiary amines were incubated over prolonged periods of time at high concentrations. Cellular uptake of the SCNPs was analyzed, presenting different uptake behavior depending on the degree of functionalization. Confocal microscopy revealed successful cytosolic delivery of SCNPs with high degrees of functionalization (45%, 60%), while SCNPs with low amounts (0% to 30%) of tertiary amines showed high degrees of colocalization with lysosomes. This work presents a strategy to direct the intracellular location of SCNPs by controlled surface modification to improve intracellular targeting for biomedical applications.

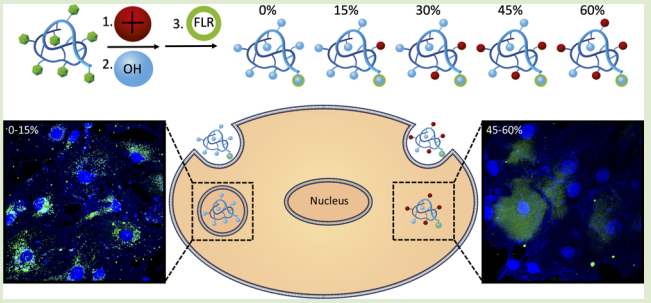

Downloaded via UNIV GRONINGEN on January 27, 2022 at 08:21:13 (UTC).
See https://pubs.acs.org/sharingguidelines for options on how to legitimately share published articles.

The field of controlled drug delivery has focused research efforts on developing nanoparticles as carriers for therapeutics,[1,2] since only a small fraction of administered therapeutics accumulates at the desired target site *in vivo*, leading to the aspiration of nanoparticles for improved treatment efficacies and decreased side effects.[3] Polymer NPs are highly modular in nature, and the ability to functionalize their surfaces is key to attaining prolonged blood circulation times and achieving targeted delivery of therapeutics to specific tissues.[4] However, a critical challenge in drug delivery is the cytosolic delivery of NPs,[3,5−7] since most therapeutics only function in specific organelles of the cell, such as in the mitochondria[8] or the cell nucleus.[9] High therapeutic effectiveness can be achieved when NPs are released from endosomal structures into the cytosol, enabling therapeutics to reach their target inside the cell.

One way to overcome this challenge of endosomal escape is by using polymers containing tertiary amines, which have been frequently utilized in nonviral gene delivery.[10−12] The buffer capacity of tertiary amines is of key importance, since after NPs are taken up by endosomes, the tertiary amines are protonated causing an influx of chloride anions.[11] The increase in ionic concentration inside the endosomes leads to osmotic swelling, which, together with the internal charge repulsion of the protonated polymers, causes the endosomes to rupture and release the cargo into the cytosol. Sprouse et al. compared the effects of various primary and tertiary amines ratios in glycopolycations for plasmid DNA delivery.[13] They observed that tertiary amines promote cellular uptake and plasmid DNA expression, which points to cytosolic delivery, although also generating cytotoxic effects. Functional groups such as guanidine, consisting of primary and secondary amines, have been successfully employed in the cytosolic delivery of NPs.[14,15] This strategy for cytosolic delivery has been adapted by Lee et al. for cytosolic protein delivery.[16] Using cationic guanidium-functionalized poly(oxanorbornene)imide (PONI) polymers of different length nanocomposites with E-tagged proteins were formed. Cytosolic delivery of these nanocomposites was confirmed; additionally longer polymers demonstrated increasing uptake.

Biodistribution and cellular uptake of polymer NPs is also further dependent on particle size. The biodistribution behavior of gold NPs with sizes ranging from 10 to 250 nm was evaluated in animal models and revealed that larger particles are mostly confined to blood, liver, and spleen, whereas smaller particles reach a variety of organs.[17,18] On the cellular level Bai et al. observed this correlation in polymer NPs ranging from 7 to 40 nm, demonstrating the highest extent of uptake for the smallest particles.[19] Due to the higher surface to

Received: August 27, 2021
Accepted: November 2, 2021
Published: November 5, 2021

ACS Publications

© 2021 The Authors. Published by American Chemical Society

volume ratio and increased curvature of smaller NPs, the contact area with membranes[20] is increased, leading to enhanced cellular uptake.[21] Access to polymer NPs smaller than 20 nm has remained limited, though intramolecular cross-linking of polymer chains provides single-chain polymer nanoparticles (SCNPs) in the 5 to 20 nm size range, in a facile and scalable manner.[22−25] Size and dispersity of SCNPs are uniquely dependent on the precursor polymers, which are readily obtained by utilizing controlled/living polymerization techniques.[26−28] The SCNPs' flexibility is between a flexible polymer and a rigid nanoparticle.[29] This combines the ability for multivalent target−ligand interactions,[30] with the increased cellular uptake seen for rigid particles.[31,32] Furthermore, SCNPs with PTR86, a targeting ligand for pancreatic cancer, have been shown to accumulate at the tumor site in a murine model, demonstrating that SCNPs can avoid fast renal clearance.[33] These characteristics have led to SCNPs being investigated in various biomedical applications, such as drug delivery,[21,34−39] targeting,[33,40] protein mimicry,[41−43] imaging,[33,44] sensing,[45] and even catalysis.[19,46,47]

Cytosolic delivery of SCNPs has so far received only limited attention. However, Liu et al. have investigated several delivery strategies for cellular uptake of SCNPs in HeLa cells.[48] PEGylated SCNPs were incubated with HeLa cells for 3 h, and the fluorescent signal of the SCNPs was observed only extracellularly. At high concentrations (2.5 mg/mL) and a relatively long 24 h incubation with SCNPs, cellular entry was observed with high degrees of colocalization with lysosomes. By making use of electroporation, the cell membrane was temporarily permeabilized and cytosolic delivery of the PEGylated SCNPs was observed. Zimmerman and co-workers designed artificial metalloenzymes for intracellular applications, and the intracellular delivery was achieved using SCNPs functionalized with quaternary ammonium cations.[47,49] In HeLa cells, colocalization with lysosomes was observed.[47] These results emphasize the demand of amines with high buffer capacity to enable the cytosolic release. In previous work, pentafluorophenyl-functional (PFP) SCNPs were synthesized via thiol-Michael addition displaying the ability for a variety of highly controlled functionalizations for biomedical applications.[43,50] PFP-SCNPs were functionalized with various peptides to develop protein mimics.

Here, we utilize controlled surface modifications to enable cytosolic delivery of SCNPs under physiologically relevant conditions, by synthesizing PFP-SCNPs, which are functionalized with increasing amounts of tertiary amines. The remaining pentafluorophenyl groups are exchanged with aminoglycerol, and a fluorescent label is conjugated for the *in vitro* analysis. Possible cytotoxic effects of the SCNPs are evaluated on mouse brain endothelial cells (bEND.3). To evaluate the uptake of the SCNPs, flow cytometry is used and the location of the SCNPs is established by confocal microscopy.

RESULTS AND DISCUSSION

Synthesis and Functionalization of SCNPs. PFP-SCNPs were prepared by slow addition of thiol-functionalized *co*-polymer to a cross-linker solution as reported earlier.[43,50] GPC analysis showed an apparent size reduction of 51% after collapse into SCNPs, indicating successful intramolecular cross-linking (Figure S1). DLS measurements showed the formation of particles with a diameter of 12 nm, with no significant larger-sized clusters present (Figure S2). Subsequently, a range of functionalized SCNPs was synthesized by conjugating the PFP-SCNPs with different ratios of the tertiary amine *N,N*-dimethylethylenediamine (DMEN) (**SCNP-0** to **SCNP-60**; see Scheme 1).

Scheme 1. Schematic Representation of SCNP Functionalization with Tertiary Amines, Alcohols, and Fluorescent Label

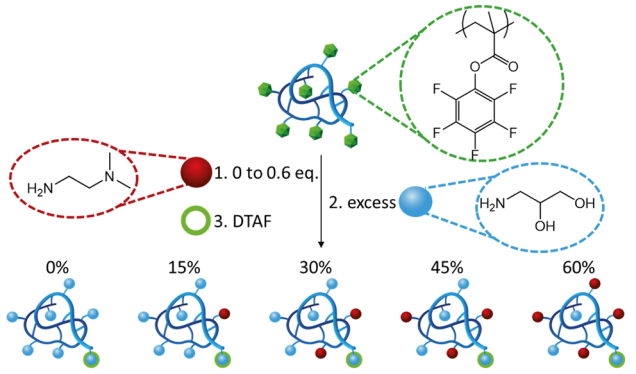

The conjugation was conveniently followed by ^{19}F NMR, indicating full conversion for all samples within 24 h (Figures S3−S7). Remaining pentafluorophenyl groups were conjugated with 1-aminoglycerol to render the SCNPs water-soluble. Incorporation of the functional groups was further evidenced by ^{1}H NMR spectroscopy (Figure S8). Signals at 2.2 ppm, corresponding to the two methyl groups attached to the tertiary amine, increased with increasing incorporation ratio, while the signals at 2.9, 3.5, and 4.5−5.0 ppm, corresponding to the incorporation of 1-aminoglycerol, diminished. The absence of signals in the ^{19}F NMR spectra (not shown) further indicates the successful formation of SCNPs with increasing amounts of tertiary amine groups. After fluorescent labeling of the SCNPs with 5-(4,6-dichlorotriazinyl) aminofluorescein (DTAF), the functionalized SCNPs were analyzed by GPC as shown in Figure S9a. The elution profiles of **SCNP-0** to **SCNP-60** show a small shift toward lower molecular mass upon higher degrees of substitution, indicating only a minor influence of the substituents on the hydrodynamic volume of the particles. Furthermore, the GPC traces confirm successful fluorescent labeling, without any significant residual free label present, which could interfere with *in vitro* experiments. Additionally, DLS measurements show particles with a comparable diameter of approximately 10 nm, while no larger aggregates are observed (Figure S10).

The surface charge of the particles was evaluated in HEPES buffer at pH 7.0 (see Figure S9b). For 0% incorporation of tertiary amines, the alcohol groups render the particles negatively charged, but upon increasing the incorporation, the SCNPs become positively charged with an apparent plateau of +27 mV for the **SCNP-60**.

Cytotoxicity of SCNPs. We previously reported that SCNPs with 1-aminoglycerol surface functionalities do not display adverse effects on the viability of human cerebral endothelial cells (hCMEC/D3).[43] However, cationic charges on the NP surface induced by protonation of tertiary amine groups are known to generate cytotoxic effects.[13,51,52] Cytotoxicity of the SCNPs was therefore evaluated on a mouse endothelial cell line (bEND.3) utilizing a resazurin assay. The cells were incubated with SCNPs over a wide

https://doi.org/10.1021/acsmacrolett.1c00558
ACS Macro Lett. 2021, 10, 1443−1449

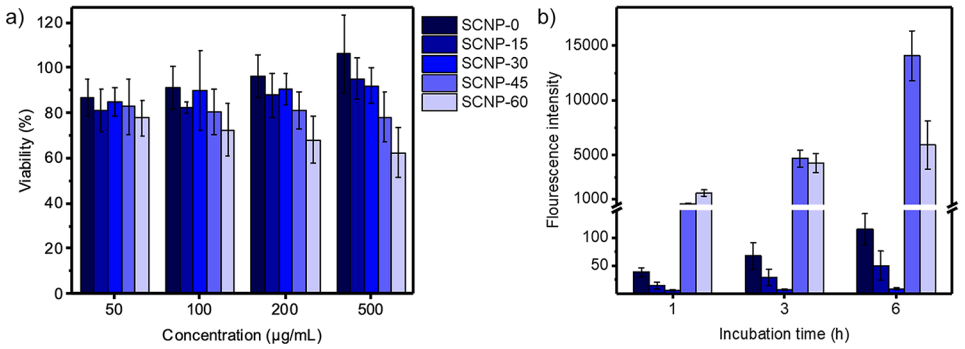

Figure 1. (a) Cell viability of bEND.3 cells after incubation with SCNPs for 24 h. (b) Fluorescence intensity of SCNPs in bEND.3 cells after 1, 3, and 6 h of incubation measured by FACS. Asterisks indicate significant higher uptake relative to **SCNP-0**, ** $p < 0.01$ and *** $p < 0.001$ ($n = 9$).

concentration range from 50 μg/mL to 500 μg/mL for 24 h. The results in Figure 1a show that **SCNP-0** to **SCNP-30** do not exert significant cytotoxic effects on the endothelial cells. At higher degrees of functionalization, however, cell viabilities decrease. For **SCNP-45** the viability decreases only when cells are exposed to an elevated concentration of 500 μg/mL, while significant toxicity for **SCNP-60** is already observed at lower concentrations. These results are in line with the results of Sprouse et al., who observed that the addition of increasing amounts of surface-located tertiary amines leads to a decrease in cell viability. Therefore, careful consideration of the density of tertiary amines on NP surfaces is key to achieving an optimal balance between high NP internalization and maintaining biocompatibility.

Cellular Uptake. Cellular uptake of the SCNPs was studied by incubating endothelial cells with the SCNPs over various time periods, followed by analysis by flow cytometry. In Figure 1b, a distinct difference in uptake behavior is observed for particles with lower ratios of tertiary amine groups on their surface (**SCNP-0**, **SCNP-15**, and **SCNP-30**) and particles with higher ratios (**SCNP-45**, **SCNP-60**) after 1 h of incubation. This disparity in uptake increases over time. For **SCNP-0** to **SCNP-30**, a slow increase in uptake is observed over time. Interestingly, **SCNP-0** displayed higher uptake than **SCNP-15** and **SCNP-30** not only after 1 h of incubation but also after longer incubation times. This implies that the interaction of particles and cell membrane is favorable for particle uptake when the particle surface is slightly negatively charged as compared to a neutral or slightly positively charged particle surface. These results are in line with the results from Xiao et al., who studied the uptake of polymer micelles with a range of surface charges.[53] The particle uptake of negatively charged NPs was higher compared to neutral NPs. They demonstrated that this effect was due to serum in the medium, which forms a protein corona that influences NP uptake,[54] as the uptake of the negatively charged and neutral particles was similar after incubation in serum-free medium.[53]

In comparison, **SCNP-45** displayed an over 10-fold higher uptake than **SCNP-0** after 1 h of incubation. Similarly enhanced uptake behavior was observed for **SCNP-60**. After prolonged incubation, **SCNP-45** shows the highest extent of internalization. Additionally, cell viabilities were evaluated utilizing a PI staining. Even for **SCNP-60** no significant cytotoxicity was observed after 1 and 6 h of incubation, in the cell populations shown in Figures S11−S12. This confirms that the tertiary amines on **SCNP-45** and **SCNP-60** only lead to decreases in cell viabilities when incubated over prolonged periods of time and high concentrations.

Intracellular Location of SCNPs. The differences in uptake behavior were further investigated by confocal microscopy. **SCNP-0** to **SCNP-30** were incubated at 50 μg/mL for 6 h, and the cells were subsequently stained with a membrane and nuclei staining. In Figure 2 the gradual decrease

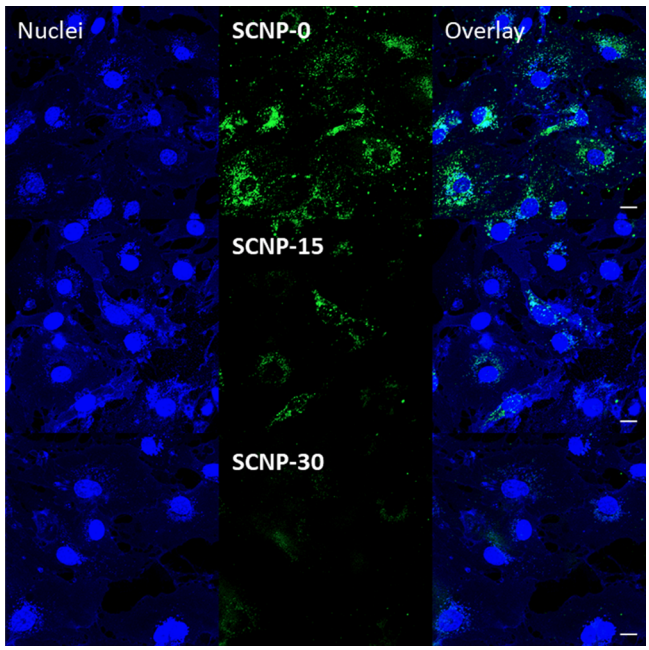

Figure 2. CLSM images of **SCNP-0**, **SCNP-15**, and **SCNP-30** uptake in bEND.3 cells after 6 h of incubation at 50 μg/mL. Nuclei and membranes were stained blue, and a green-fluorescent label was used on the SCNPs, scale bar 10 μm.

of green signal from **SCNP-0** to **SCNP-30** can be observed, confirming the increase in uptake for negatively charged **SCNP-0** as compared to **SCNP-30**, as measured by flow cytometry. Furthermore, the fluorescent signal of SCNPs is observed in vesicle structures inside the cells. These results resemble the uptake behavior of glycerol-SCNPs shown in previous work, indicating endosomal uptake.[37]

As described above, high uptake rates were observed for **SCNP-45** and **SCNP-60**. Therefore, these particles were incubated for only 1 h at 50 μg/mL with bEND.3 cells for confocal microscopy. Subsequently, the cells were stained with membrane and nuclei staining. In contrast to **SCNP-0** to **SCNP-30**, less SCNPs in vesicle structures were observed for **SCNP-45**. Instead, the signal of the SCNPs is observed in the

https://doi.org/10.1021/acsmacrolett.1c00558
ACS Macro Lett. 2021, 10, 1443−1449

cytosol shown in Figure 3. In gene[13,55] and protein[5,56] delivery, polymers with tertiary amines are utilized to form complexes

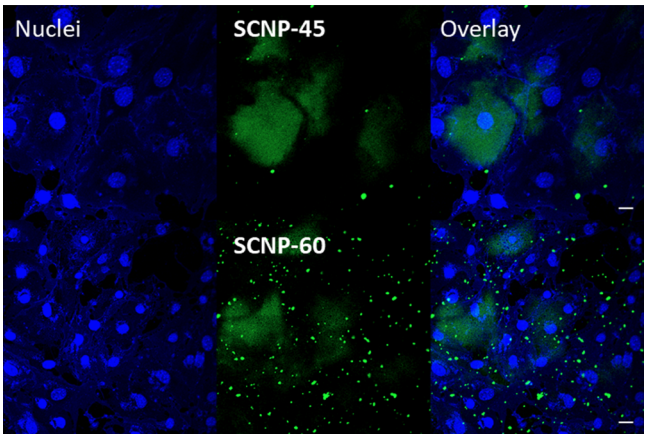

Figure 3. CLSM images of **SCNP-45** and **SCNP-60** uptake in bEND.3 cells after 1 h of incubation at 50 μg/mL. Nuclei and membranes were stained blue, and a green-fluorescent label was used on the SCNPs, scale bar 10 μm.

with negatively charged cargoes, to deliver the cargo in the cytosol of cells exploiting the proton sponge effect. In line with these studies, amine moieties of the SCNPs become protonated at the endosomal/lysosomal pH increasing the internal pressure after internalization. With increasing surface functionality of the SCNPs, the pressure increases, leading to lysing of the endosomes and endosomal escape for **SCNP-45**. For **SCNP-60** the cytosolic delivery is also observed, but additional signals corresponding to aggregated SCNPs are also observed (see Figure 3).

In the analysis of the location of SCNPs in the bEND.3 cells, **SCNP-0** to **SCNP-30** were incubated with cells for 6 h. Subsequently, the lysosomes were stained. In Figure 4, particle uptake and colocalization with lysosomes are shown. High degrees of colocalization for **SCNP-0** and **SCNP-15** with the lysosomes were observed. Additionally, green signals corresponding to **SCNP-0** inside vesicle structures were observed. As shown earlier, less internalization of **SCNP-30** was visible, and the signal colocalized partly with lysosomes. While this uptake behavior is not favorable for drug delivery in most applications, as encapsulated therapeutics do not reach the cytosol efficiently,[10] these results are interesting for applications in which NPs rather have to cross a cell barrier. For example in drug delivery to the brain, NPs have to cross the blood–brain barrier (BBB) to reach the target.[57] In this highly selective process, NPs are taken up by cells and have to achieve transcytosis to enter the brain. The particles are dependent on the intracellular vesicular trafficking, which directs particles that are taken up by endocytosis toward lysosomes, recycling endosomes, which release the particles back into the bloodstream or transcystosis.[58] Bannunah and co-workers investigated the influence of NP charge and size on the internalization and crossing of an intestinal epithelial cell model.[52] They reported higher uptake for positively charged NP. However, the transport across the cell barrier was higher for negatively charged NPs. Further research of the negative or neutral surface charged SCNPs could demonstrate what surface charge is optimal to cross cell barriers, such as the BBB.

SCNP-45 and **SCNP-60** were incubated for 30 min with bEND.3 cells before the lysosomes were stained. In Figure 5,

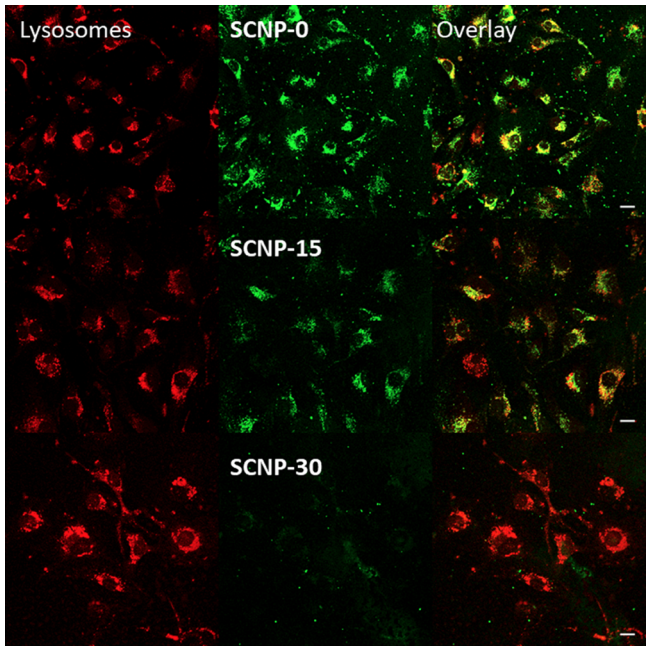

Figure 4. CLSM images of bEND.3 cells incubated with **SCNP-0**, **SCNP-15**, and **SCNP-30** for 6 h and stained with Lysotracker, scale bar 10 μm.

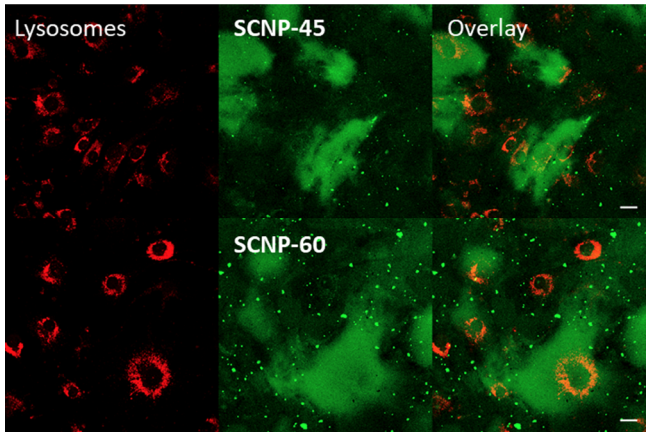

Figure 5. CLSM images of bEND.3 cells treated with **SCNP-45** and **SCNP-60** for 30 min and Lysotracker, scale bar 10 μm.

the green signal from **SCNP-45** and **SCNP-60** was observed throughout the cells confirming successful cytosolic delivery. Furthermore, some intracellular aggregation of **SCNP-45** and **SCNP-60** was observed as well at shorter incubation time, as compared to the uptake study. However, the lysosome staining does not colocalize with the particle aggregations, indicating that the particles partly form intracellular clusters.

CONCLUSIONS

In this work, PFP-SCNPs were synthesized and subsequently functionalized with tertiary amines to induce a positive surface charge under physiological conditions. The zeta-potential of the SCNPs increased with higher degrees of functionalization, while particle size remained constant. This range of SCNPs enabled investigation of their cellular interactions, only in relation to the degree of functionalization. None of the SCNPs exerts significant cytotoxicity after 6 h incubation on bEND.3 cells. The SCNPs with high amounts of tertiary amines only

https://doi.org/10.1021/acsmacrolett.1c00558
ACS Macro Lett. 2021, 10, 1443−1449

caused minor cytotoxicity at high concentrations coupled with long incubation times. However, all SCNPs show cellular uptake at low particle concentrations, which have been shown to be biocompatible. The highest cellular uptake was observed for **SCNP-45**, in which 45% of the monomer units possess a protonable tertiary amine. Significant differences in uptake behavior were observed for **SCNP-0** to **-30** and **SCNP-45** and **-60**. At lower degrees of functionalization (0−30%), cellular uptake remained low, while, at 45−60% of functionalization, uptake increased by up to 2 orders of magnitude. Confocal microscopy revealed successful cytosolic delivery of **SCNP-45** and **SCNP-60**. As shown with a lysosome staining for **SCNP-0** to **SCNP-30**, the majority of SCNPs end up in lysosomes and the higher amounts of tertiary amines in **SCNPs-45** and **SCNP-60** were sufficient to increase the ionic concentration inside the endosome, promoting endosomal escape. This systematic study shows the importance of controlled surface functionalization, as minor changes in the amounts of tertiary amines can already affect uptake rate and even intracellular location. The introduction of new and more specific targeting ligands can further increase the selectivity of SCNP targeting. These versatile SCNPs provide a platform for various drug delivery applications, as the surface modification enables directing the delivery to different subcellular targets, importantly including the cytosol and thereby increasing the efficacy of therapeutics. The control and ease of functionalization contribute to the ability to rapidly adapt SCNPs for therapeutic translation.

■ ASSOCIATED CONTENT

Supporting Information

The Supporting Information is available free of charge at https://pubs.acs.org/doi/10.1021/acsmacrolett.1c00558.

Materials and Methods, DLS/GPC data, ^{19}F and ^{1}H NMR spectra, and FACS data. (PDF)

■ AUTHOR INFORMATION

Corresponding Author

Jos M. J. Paulusse − *Department of Molecules and Materials, MESA+ Institute for Nanotechnology and TechMed Institute for Health and Biomedical Technologies, Faculty of Science and Technology, University of Twente, 7500 AE Enschede, The Netherlands; Department of Nuclear Medicine and Molecular Imaging, University Medical Center Groningen, 9700 RB Groningen, The Netherlands;* orcid.org/0000-0003-0697-7202; Email: J.M.J.Paulusse@utwente.nl

Authors

Naomi M. Hamelmann − *Department of Molecules and Materials, MESA+ Institute for Nanotechnology and TechMed Institute for Health and Biomedical Technologies, Faculty of Science and Technology, University of Twente, 7500 AE Enschede, The Netherlands;* orcid.org/0000-0002-7126-4818

Jan-Willem D. Paats − *Department of Molecules and Materials, MESA+ Institute for Nanotechnology and TechMed Institute for Health and Biomedical Technologies, Faculty of Science and Technology, University of Twente, 7500 AE Enschede, The Netherlands*

Complete contact information is available at: https://pubs.acs.org/10.1021/acsmacrolett.1c00558

Notes

The authors declare no competing financial interest.

■ ACKNOWLEDGMENTS

The funding from Health−Holland, Top Sector Life Science & Health, to stimulate public-private partnership, the Euro-NanoMed III research program (ref. EURO-NANO-MED2017-178), and Alzheimer Netherlands is gratefully acknowledged.

■ REFERENCES

(1) Hoffman, A. S. The origins and evolution of "controlled" drug delivery systems. *J. Controlled Release* **2008**, *132* (3), 153−163.

(2) Park, K. Controlled drug delivery systems: Past forward and future back. *J. Controlled Release* **2014**, *190*, 3−8.

(3) Torchilin, V. P.; Levchenko, T. S. TAT-liposomes: a novel intracellular drug carrier. *Curr. Protein Pept. Sci.* **2003**, *4* (2), 133−40.

(4) Ye, F.; Ke, T.; Jeong, E.-K.; Wang, X.; Sun, Y.; Johnson, M.; Lu, Z.-R. Noninvasive Visualization of in Vivo Drug Delivery of Poly(l-glutamic acid) Using Contrast-Enhanced MRI. *Mol. Pharmaceutics* **2006**, *3* (5), 507−515.

(5) Vasir, J. K.; Labhasetwar, V. Biodegradable nanoparticles for cytosolic delivery of therapeutics. *Adv. Drug Delivery Rev.* **2007**, *59* (8), 718−728.

(6) Tang, R.; Jiang, Z.; Ray, M.; Hou, S.; Rotello, V. M. Cytosolic delivery of large proteins using nanoparticle-stabilized nanocapsules. *Nanoscale* **2016**, *8* (42), 18038−18041.

(7) Galliani, M.; Tremolanti, C.; Signore, G. Nanocarriers for Protein Delivery to the Cytosol: Assessing the Endosomal Escape of Poly(Lactide-co-Glycolide)-Poly(Ethylene Imine) Nanoparticles. *Nanomaterials* **2019**, *9* (4), 652.

(8) Letai, A.; Bassik, M. C.; Walensky, L. D.; Sorcinelli, M. D.; Weiler, S.; Korsmeyer, S. J. Distinct BH3 domains either sensitize or activate mitochondrial apoptosis, serving as prototype cancer therapeutics. *Cancer Cell* **2002**, *2* (3), 183−192.

(9) Yao, J.; Fan, Y.; Li, Y.; Huang, L. Strategies on the nuclear-targeted delivery of genes. *J. Drug Target.* **2013**, *21* (10), 926−939.

(10) Degors, I. M. S.; Wang, C.; Rehman, Z. U.; Zuhorn, I. S. Carriers Break Barriers in Drug Delivery: Endocytosis and Endosomal Escape of Gene Delivery Vectors. *Acc. Chem. Res.* **2019**, *52* (7), 1750−1760.

(11) Vermeulen, L. M. P.; De Smedt, S. C.; Remaut, K.; Braeckmans, K. The proton sponge hypothesis: Fable or fact? *Eur. J. Pharm. Biopharm.* **2018**, *129*, 184−190.

(12) Wattiaux, R.; Laurent, N.; Wattiaux-De Coninck, S.; Jadot, M. Endosomes, lysosomes: their implication in gene transfer. *Adv. Drug Delivery Rev.* **2000**, *41* (2), 201−208.

(13) Sprouse, D.; Reineke, T. M. Investigating the Effects of Block versus Statistical Glycopolycations Containing Primary and Tertiary Amines for Plasmid DNA Delivery. *Biomacromolecules* **2014**, *15* (7), 2616−2628.

(14) Wender, P. A.; Galliher, W. C.; Goun, E. A.; Jones, L. R.; Pillow, T. H. The design of guanidinium-rich transporters and their internalization mechanisms. *Adv. Drug Delivery Rev.* **2008**, *60* (4−5), 452−472.

(15) Hamilton, S. K.; Harth, E. Molecular Dendritic Transporter Nanoparticle Vectors Provide Efficient Intracellular Delivery of Peptides. *ACS Nano* **2009**, *3* (2), 402−410.

(16) Lee, Y.-W.; Luther, D. C.; Goswami, R.; Jeon, T.; Clark, V.; Elia, J.; Gopalakrishnan, S.; Rotello, V. M. Direct Cytosolic Delivery of Proteins through Coengineering of Proteins and Polymeric Delivery Vehicles. *J. Am. Chem. Soc.* **2020**, *142* (9), 4349−4355.

(17) De Jong, W. H.; Hagens, W. I.; Krystek, P.; Burger, M. C.; Sips, A. J. A. M.; Geertsma, R. E. Particle size-dependent organ distribution of gold nanoparticles after intravenous administration. *Biomaterials* **2008**, *29* (12), 1912−1919.

(18) Sonavane, G.; Tomoda, K.; Makino, K. Biodistribution of colloidal gold nanoparticles after intravenous administration: Effect of particle size. *Colloids Surf., B* **2008**, *66* (2), 274−280.
(19) Bai, Y.; Xing, H.; Wu, P.; Feng, X.; Hwang, K.; Lee, J. M.; Phang, X. Y.; Lu, Y.; Zimmerman, S. C. Chemical Control over Cellular Uptake of Organic Nanoparticles by Fine Tuning Surface Functional Groups. *ACS Nano* **2015**, *9* (10), 10227−10236.
(20) Bahrami, A. H.; Raatz, M.; Agudo-Canalejo, J.; Michel, R.; Curtis, E. M.; Hall, C. K.; Gradzielski, M.; Lipowsky, R.; Weikl, T. R. Wrapping of nanoparticles by membranes. *Adv. Colloid Interface Sci.* **2014**, *208*, 214−224.
(21) Chen, X.; Li, R.; Wong, S. H. D.; Wei, K.; Cui, M.; Chen, H.; Jiang, Y.; Yang, B.; Zhao, P.; Xu, J.; Chen, H.; Yin, C.; Lin, S.; Lee, W. Y.-W.; Jing, Y.; Li, Z.; Yang, Z.; Xia, J.; Chen, G.; Li, G.; Bian, L. Conformational manipulation of scale-up prepared single-chain polymeric nanogels for multiscale regulation of cells. *Nat. Commun.* **2019**, *10* (1), 2705.
(22) Kröger, A. P. P.; Paulusse, J. M. J. Single-chain polymer nanoparticles in controlled drug delivery and targeted imaging. *J. Controlled Release* **2018**, *286*, 326−347.
(23) Gonzalez-Burgos, M.; Latorre-Sanchez, A.; Pomposo, J. A. Advances in single chain technology. *Chem. Soc. Rev.* **2015**, *44* (17), 6122−6142.
(24) Harth, E.; Horn, B. V.; Lee, V. Y.; Germack, D. S.; Gonzales, C. P.; Miller, R. D.; Hawker, C. J. A Facile Approach to Architecturally Defined Nanoparticles via Intramolecular Chain Collapse. *J. Am. Chem. Soc.* **2002**, *124* (29), 8653−8660.
(25) Seo, M.; Beck, B. J.; Paulusse, J. M. J.; Hawker, C. J.; Kim, S. Y. Polymeric Nanoparticles via Noncovalent Cross-Linking of Linear Chains. *Macromolecules* **2008**, *41* (17), 6413−6418.
(26) Braunecker, W. A.; Matyjaszewski, K. Controlled/living radical polymerization: Features, developments, and perspectives. *Prog. Polym. Sci.* **2007**, *32* (1), 93−146.
(27) Moad, G.; Barner-Kowollik, C. The Mechanism and Kinetics of the RAFT Process: Overview, Rates, Stabilities, Side Reactions, Product Spectrum and Outstanding Challenges. *In Handbook of RAFT Polymerization* **2008**, 51−104.
(28) Moad, G.; Rizzardo, E.; Thang, S. H. Living Radical Polymerization by the RAFT Process - A Third Update. *Aust. J. Chem.* **2012**, *65* (8), 985−1076.
(29) Pomposo, J. A.; Perez-Baena, I.; Lo Verso, F.; Moreno, A. J.; Arbe, A.; Colmenero, J. How Far Are Single-Chain Polymer Nanoparticles in Solution from the Globular State? *ACS Macro Lett.* **2014**, *3* (8), 767−772.
(30) Woythe, L.; Tito, N. B.; Albertazzi, L. A quantitative view on multivalent nanomedicine targeting. *Adv. Drug Delivery Rev.* **2021**, *169*, 1−21.
(31) Sun, J.; Zhang, L.; Wang, J.; Feng, Q.; Liu, D.; Yin, Q.; Xu, D.; Wei, Y.; Ding, B.; Shi, X.; Jiang, X. Tunable Rigidity of (Polymeric Core)-(Lipid Shell) Nanoparticles for Regulated Cellular Uptake. *Adv. Mater.* **2015**, *27* (8), 1402−1407.
(32) Wang, S.; Guo, H.; Li, Y.; Li, X. Penetration of nanoparticles across a lipid bilayer: effects of particle stiffness and surface hydrophobicity. *Nanoscale* **2019**, *11* (9), 4025−4034.
(33) Benito, A. B.; Aiertza, M. K.; Marradi, M.; Gil-Iceta, L.; Shekhter Zahavi, T.; Szczupak, B.; Jiménez-González, M.; Reese, T.; Scanziani, E.; Passoni, L.; Matteoli, M.; De Maglie, M.; Orenstein, A.; Oron-Herman, M.; Kostenich, G.; Buzhansky, L.; Gazit, E.; Grande, H.-J.; Gómez-Vallejo, V.; Llop, J.; Loinaz, I. Functional Single-Chain Polymer Nanoparticles: Targeting and Imaging Pancreatic Tumors in Vivo. *Biomacromolecules* **2016**, *17* (10), 3213−3221.
(34) Song, C.; Li, L.; Dai, L.; Thayumanavan, S. Responsive single-chain polymer nanoparticles with host-guest features. *Polym. Chem.* **2015**, *6* (26), 4828−4834.
(35) Gracia, R.; Marradi, M.; Cossío, U.; Benito, A.; Pérez-San Vicente, A.; Gómez-Vallejo, V.; Grande, H. J.; Llop, J.; Loinaz, I. Synthesis and functionalization of dextran-based single-chain nanoparticles in aqueous media. *J. Mater. Chem. B* **2017**, *5* (6), 1143−1147.
(36) Gracia, R.; Marradi, M.; Salerno, G.; Pérez-Nicado, R.; Pérez-San Vicente, A.; Dupin, D.; Rodriguez, J.; Loinaz, I.; Chiodo, F.; Nativi, C. Biocompatible single-chain polymer nanoparticles loaded with an antigen mimetic as potential anticancer vaccine. *ACS Macro Lett.* **2018**, *7* (2), 196−200.
(37) Kröger, A. P. P.; Hamelmann, N. M.; Juan, A.; Lindhoud, S.; Paulusse, J. M. J. Biocompatible Single-Chain Polymer Nanoparticles for Drug Delivery—A Dual Approach. *ACS Appl. Mater. Interfaces* **2018**, *10* (37), 30946−30951.
(38) Asenjo-Sanz, I.; Del-Corte, M.; Pinacho-Olaciregui, J.; González-Burgos, M.; González, E.; Verde-Sesto, E.; Arbe, A.; Colmenero, J.; Pomposo, J. A. Preparation and Preliminary Evaluation of Povidone Single-Chain Nanoparticles as Potential Drug Delivery Nanocarriers. *Med. One* **2019**, *4* (4), No. e190013.
(39) Madeira do O, J.; Foralosso, R.; Yilmaz, G.; Mastrotto, F.; King, P. J. S.; Xerri, R. M.; He, Y.; van der Walle, C. F.; Fernandez-Trillo, F.; Laughton, C. A.; Styliari, I.; Stolnik, S.; Mantovani, G. Poly(triazolyl methacrylate) glycopolymers as potential targeted unimolecular nanocarriers. *Nanoscale* **2019**, *11* (44), 21155−21166.
(40) Kröger, A. P. P.; Komil, M. I.; Hamelmann, N. M.; Juan, A.; Stenzel, M. H.; Paulusse, J. M. J. Glucose Single-Chain Polymer Nanoparticles for Cellular Targeting. *ACS Macro Lett.* **2019**, *8* (1), 95−101.
(41) Perez-Baena, I.; Barroso-Bujans, F.; Gasser, U.; Arbe, A.; Moreno, A. J.; Colmenero, J.; Pomposo, J. A. Endowing Single-Chain Polymer Nanoparticles with Enzyme-Mimetic Activity. *ACS Macro Lett.* **2013**, *2* (9), 775−779.
(42) Huo, M.; Wang, N.; Fang, T.; Sun, M.; Wei, Y.; Yuan, J. Single-chain polymer nanoparticles: Mimic the proteins. *Polymer* **2015**, *66*, A11−A21.
(43) Kröger, A. P. P.; Paats, J.-W. D.; Boonen, R. J. E. A.; Hamelmann, N. M.; Paulusse, J. M. J. Pentafluorophenyl-based single-chain polymer nanoparticles as a versatile platform towards protein mimicry. *Polym. Chem.* **2020**, *11* (37), 6056−6065.
(44) Hoffmann, J. F.; Roos, A. H.; Schmitt, F. J.; Hinderberger, D.; Binder, W. H. Fluorescent and Water Dispersible Single-Chain Nanoparticles: Core-Shell Structured Compartmentation. *Angew. Chem., Int. Ed.* **2021**, *60*, 7820−7827.
(45) Gillissen, M. A. J.; Voets, I. K.; Meijer, E. W.; Palmans, A. R. A. Single chain polymeric nanoparticles as compartmentalised sensors for metal ions. *Polym. Chem.* **2012**, *3* (11), 3166−3174.
(46) Liu, Y.; Turunen, P.; de Waal, B. F. M.; Blank, K. G.; Rowan, A. E.; Palmans, A. R. A.; Meijer, E. W. Catalytic single-chain polymeric nanoparticles at work: from ensemble towards single-particle kinetics. *Molecular Systems Design & Engineering* **2018**, *3* (4), 609−618.
(47) Chen, J.; Li, K.; Shon, J. S. L.; Zimmerman, S. C. Single-Chain Nanoparticle Delivers a Partner Enzyme for Concurrent and Tandem Catalysis in Cells. *J. Am. Chem. Soc.* **2020**, *142* (10), 4565−4569.
(48) Liu, Y.; Pujals, S.; Stals, P. J. M.; Paulöhrl, T.; Presolski, S. I.; Meijer, E. W.; Albertazzi, L.; Palmans, A. R. A. Catalytically Active Single-Chain Polymeric Nanoparticles: Exploring Their Functions in Complex Biological Media. *J. Am. Chem. Soc.* **2018**, *140* (9), 3423−3433.
(49) Chen, J.; Wang, J.; Li, K.; Wang, Y.; Gruebele, M.; Ferguson, A. L.; Zimmerman, S. C. Polymeric "Clickase" Accelerates the Copper Click Reaction of Small Molecules, Proteins, and Cells. *J. Am. Chem. Soc.* **2019**, *141* (24), 9693−9700.
(50) Kröger, A. P. P.; Boonen, R. J. E. A.; Paulusse, J. M. J. Well-defined single-chain polymer nanoparticles via thiol-Michael addition. *Polymer* **2017**, *120*, 119−128.
(51) Naha, P. C.; Davoren, M.; Lyng, F. M.; Byrne, H. J. Reactive oxygen species (ROS) induced cytokine production and cytotoxicity of PAMAM dendrimers in J774A.1 cells. *Toxicol. Appl. Pharmacol.* **2010**, *246* (1), 91−99.
(52) Bannunah, A. M.; Vllasaliu, D.; Lord, J.; Stolnik, S. Mechanisms of nanoparticle internalization and transport across an intestinal epithelial cell model: effect of size and surface charge. *Mol. Pharmaceutics* **2014**, *11* (12), 4363−73.

https://doi.org/10.1021/acsmacrolett.1c00558
ACS Macro Lett. 2021, 10, 1443−1449

(53) Xiao, K.; Li, Y.; Luo, J.; Lee, J. S.; Xiao, W.; Gonik, A. M.; Agarwal, R. G.; Lam, K. S. The effect of surface charge on in vivo biodistribution of PEG-oligocholic acid based micellar nanoparticles. *Biomaterials* **2011**, *32* (13), 3435−3446.
(54) Ke, P. C.; Lin, S.; Parak, W. J.; Davis, T. P.; Caruso, F. A Decade of the Protein Corona. *ACS Nano* **2017**, *11* (12), 11773−11776.
(55) Pack, D. W.; Hoffman, A. S.; Pun, S.; Stayton, P. S. Design and development of polymers for gene delivery. *Nat. Rev. Drug Discovery* **2005**, *4* (7), 581−593.
(56) Goswami, R.; Jeon, T.; Nagaraj, H.; Zhai, S.; Rotello, V. M. Accessing Intracellular Targets through Nanocarrier-Mediated Cytosolic Protein Delivery. *Trends Pharmacol. Sci.* **2020**, *41* (10), 743−754.
(57) Pulgar, V. M. Transcytosis to Cross the Blood Brain Barrier, New Advancements and Challenges. *Front. Neurosci.* **2019**, *12*, 1019.
(58) Toth, A. E.; Nielsen, S. S. E.; Tomaka, W.; Abbott, N. J.; Nielsen, M. S. The endo-lysosomal system of bEnd.3 and hCMEC/D3 brain endothelial cells. *Fluids Barriers CNS* **2019**, *16* (1), 14.

https://doi.org/10.1021/acsmacrolett.1c00558
ACS Macro Lett. 2021, 10, 1443−1449